Electron Transfer Kinetics during the Reduction and Turnover of the Cytochrome caa_3 Complex from *Bacillus subtilis*†

Mahmoud Assempour, Dan Lim, and Bruce C. Hill*

Department of Biochemistry, Queen's University, Kingston, Ontario, K7L 3N6 Canada

Received February 10, 1998; Revised Manuscript Received May 6, 1998

ABSTRACT: The cytochrome caa_3 complex from *Bacillus subtilis* is a member of the cytochrome oxidase superfamily of respiratory enzyme complexes. The key difference in the cytochrome caa_3 complex lies in the addition of a domain, homologous with mitochondrial cytochrome *c*, that is fused to the C-terminal end of its subunit II. Measurements of steady-state and transient reduction kinetics have been carried out on the cytochrome caa_3 complex. Reduction of the cyanide-bound enzyme with ascorbate and *N*,*N*,*N*′,*N*′-tetramethyl-*p*-phenylenediamine (TMPD) supports a sequence of electron transfer in which cytochrome *c* is reduced initially, and this is followed by rapid internal electron transfer from cytochrome *c* to Cu_A and from Cu_A to cytochrome *a*. Steady-state kinetics with exogenous cytochrome *c* as the substrate demonstrates the capability of the cytochrome caa_3 complex to act as a cytochrome *c* oxidase. The cytochrome *c* from *B. subtilis* is the most efficient cytochrome *c* of those tested. Steady-state kinetics with ascorbate−TMPD as the reductant, in the absence of exogenous cytochrome *c*, reveals a biphasic pattern even though only a single, covalent cytochrome *c* interaction site is present. The two-phase kinetics are characterized by a low activity phase associated with a high apparent affinity for TMPD and a high activity phase with a low affinity for TMPD. This pattern is observed over a wide range of ionic strengths and enzyme concentrations, and with both purified and membrane extract forms of cytochrome caa_3. It is proposed that the biphasic steady-state kinetics of this oxidase, and other members of the cytochrome oxidase superfamily, do not result directly from different interactions with cytochrome *c* but are due to a change in the redox kinetics within the centers of the conventional oxidase unit itself. Our results will be related to models that account for the biphasic steady-state kinetics exhibited by cytochrome oxidase.

Cytochrome oxidase is an integral membrane enzyme that is the terminal member of many respiratory chains in a wide variety of aerobic organisms. The enzyme catalyzes the delivery of electrons and protons to molecular oxygen to produce water. Some of the free energy of the redox process is conserved by the coupling of transmembrane proton movement to generate an electrochemical potential in a process that is tightly coupled to the electron-transfer reaction catalyzed by the oxidase (*1*). This transmembrane electrochemical disequilibrium is utilized by energy-requiring reactions, such as the synthesis of ATP catalyzed by the proton-linked ATP synthase complex.

A superfamily of homologous cytochrome oxidase enzyme complexes has been recognized (*2*) as have two subfamilies that differ in their use of reducing substrates. There is the class, represented by mitochondrial cytochrome oxidase, that uses ferrocytochrome *c* as a reducing substrate, and they are referred to as cytochrome *c* oxidases. The second class uses, instead of cytochrome *c*, a quinol as a reducing substrate, and they are known as quinol oxidases. Classical cytochrome *c* oxidases, of which the bovine heart mitochondrial enzyme is the best-studied, possess five redox active metal ions that are arranged in three centers: Cu_A, cytochrome *a*, and cytochrome a_3-Cu_B (*3*). Cu_A contains two copper ions forming a dinuclear site bound to a set of six residues within subunit II. Cu_A accepts one electron in its transition from oxidized to reduced, although its potential capacity is greater. Cytochrome *a* is bound by two histidine residues in subunit I that occupy the axial ligand positions to the heme iron, and it acts as a single electron carrier. A second heme A group and another copper atom form a binuclear site, cytochrome a_3-Cu_B. Cytochrome a_3-Cu_B is the site where the enzyme reacts with oxygen and is also proposed to be intimately involved in coupling electron transfer to transmembrane proton movement which is necessary for energy conservation (*4*, *5*).

A subgrouping of enzyme complexes within the cytochrome *c* oxidases are those that have a cytochrome *c* domain fused into the sequence of subunit II, an otherwise well-conserved oxidase subunit. Cytochrome caa_3 complexes have the three metal centers of classical cytochrome *c* oxidase and an additional metal, the heme center of the cytochrome *c* domain. This extra domain includes the canonical sequence for attachment of a heme C group and is overall homologous in sequence to mammalian cytochrome *c*. Such cytochrome caa_3 complexes are found in bacteria such as *Bacillus subtilis* (*6*), *Bacillus* sp. PS3 (*7*), *Thermus thermophilus* (*8*), and *Bacillus firmus* (*9*). The cytochrome caa_3 complex from *B. subtilis* is the subject of the work described in this paper.

† Supported by an operating grant from the Medical Research Council (Canada) to B.C.H.

* To whom correspondence should be addressed.

S0006-2960(98)00331-6 CCC: $15.00
Published on Web 06/19/1998

Transient kinetic studies of the reaction of fully reduced mitochondrial oxidase with O_2 have led to a model of the sequence of individual electron-transfer reactions within the oxidase (*10*−*12*). Some of the individual steps in this sequence have been supported by the results from additional transient kinetic experiments using reverse electron transfer following photodissociation (*13*, *14*) and photoreductive kinetic studies with ruthenium compounds alone (*15*) or as derivatives of photoreducible cytochrome *c* (*16*, *17*). It is proposed that electron input to cytochrome *c* oxidase from ferrocytochrome *c* happens exclusively via the Cu_A center in subunit II. Electrons flow from Cu_A to cytochrome *a* in subunit I, and then to the cytochrome a_3−Cu_B center where O_2 binding and reduction occur. Recent transient-state kinetic studies on the single-turnover reaction of reduced *B. subtilis* cytochrome caa_3 with oxygen (*18*) have shown a reactivity very similar to that reported for the eukaryotic cytochrome *c*−cytochrome *c* oxidase complex formed at low ionic strengths (*19*). How the above sequence of reactions is related to the steady-state turnover of cytochrome *c* oxidase is not understood.

Steady-state kinetic studies of mitochondrial cytochrome *c* oxidase as a function of cytochrome *c* concentration reveal two phases in the enzyme's activity that reflect a negative cooperativity in affinity for cytochrome *c* and positive cooperativity in molecular activity as the cytochrome *c* concentration is increased. This behavior has been interpreted in a number of ways (*20*). It has been described as arising from two distinct binding sites of high and low affinity for cytochrome *c* that are associated with low and high activity, respectively (*21*). An alternative view is that the biphasic behavior results from distinct but interconverting forms of cytochrome *c* oxidase. In this model, the enzyme is viewed as having one physical site for binding cytochrome *c*, but the enzyme takes up two different conformations with vastly different maximal molecular activities (*22*).

In our work, we have pursued the study of cytochrome caa_3 from *B. subtilis* to assess its suitability as a model for the cytochrome *c*−cytochrome *c* oxidase complex that is stable at low ionic strengths and forms, at least transiently, in the steady-state turnover cycle of mitochondrial cytochrome *c* oxidase. We find that the transient-state reduction kinetics of cyanide-inhibited cytochrome caa_3 resemble those found previously for the electrostatic complex formed between mitochondrial cytochrome *c* and cytochrome *c* oxidase (*23*). The *B. subtilis* caa_3 complex is able to oxidize exogenous cytochrome *c*, but with only low affinity as though the covalently attached cytochrome *c* domain occupies what would be the high-affinity site of the mitochondrial enzyme. The activity of the cytochrome caa_3 complex from *B. subtilis* is maximal with the electron donors ascorbate and TMPD.[1] The rate of this reaction is largely independent of ionic strength and has allowed studies using up to 250 mM ascorbate. Under these conditions, the steady state of cytochrome *c* can approach 100% reduction at high rates of flux. The enzyme exhibits biphasic steady-state behavior as a function of TMPD concentration that is reminiscent of the mitochondrial oxidase activity in response to cytochrome *c* concentration. We propose that this biphasic steady-state behavior of cytochrome oxidases in general is not due to different interactions with cytochrome *c* but is an intrinsic property of the oxidase.

MATERIALS AND METHODS

The cytochrome caa_3 complex from *B. subtilis* was purified according to the procedure outlined by Henning et al. (*24*) with the following modification. The initial hydroxylapatite column was replaced by a Ni-containing metal affinity column (Chelating Sepharose, Pharmacia, Pointe Claire, PQ). This is then followed by the use of a sequence of cation and anion exchange columns as described previously (*24*). A final heme-to-protein ratio of 18−20 nmol of heme A per milligram of protein is obtained. *B. subtilis* cytochrome *c* was purified from an overexpressing strain to a give a heme-to-protein ratio of >40 nmol of heme C per milligram of protein and a single Coomassie-stained band on SDS−polyacrylamide gels (P. S. David and B. C. Hill, in preparation).

The oxidation of exogenous, reduced cytochrome *c* was measured spectrophotometrically using the intensity of the absorbance at 550−540 nm. Cytochrome *c* samples were reduced by incubation with an excess of sodium ascorbate followed by gel filtration on G-25 to remove the reductant. The assay medium was 25 mM sodium phosphate (pH 7.0) with 1 mM EDTA and 0.5 mg/mL lauryl maltoside. Observed rates were calculated from the half-times of the absorbance profiles and velocities determined by multiplying the observed rate by the cytochrome *c* concentration (*25*). TN_{max} and K_M values were determined for *B. subtilis* and *Pseudomonas aeruginosa* cytochromes *c* by fitting the velocity versus substrate concentration data to a rectangular hyperbola.

Steady-state activity measurements made polarographically were taken using an oxygen electrode from Rank Brothers (Mono Research Laboratories, Brampton, ON). The output from the electrode was recorded, and the rates were read off the chart as micromoles of oxygen per minute. The background rate of ascorbate and TMPD oxidation in the absence of the enzyme was subtracted from the enzyme-catalyzed rate. Steady-state activity was also measured spectrophotometrically using a Hewlett-Packard diode array spectrophotometer interfaced to a Hi-tech SF-12 rapid mixing module. For this method, the reduction level of the enzyme was assessed during steady-state turnover. The time taken to consume all of the oxygen in the cuvette, or the anerobiosis time, was assessed by the sudden change in absorbance level as the enzyme moves from steady-state reduction to full reduction. This time is then used to calculate a rate of oxygen consumption. A key difference between these two assay modes is in the level of enzyme present. The polarographic assay is carried out typically with 25−50 nM enzyme, whereas the spectrophotometric assay is carried out with 100-fold more enzyme to observe the spectra of the cytochrome components directly.

UV−visible spectra were recorded on either a Shimadzu UV-160 or a Hewlett-Packard HP8452 spectrophotometer. Measurements of transient reduction kinetics were performed using a locally constructed spectrometer composed of a Bio-Logic SFM3 stopped-flow cell coupled to an optical bench

[1] Abbreviations: UV, ultraviolet; CD, circular dichroism; EDTA, ethylenediaminetetraacetic acid; FTIR, Fourier transform infrared; TMPD, *N*,*N*,*N*′,*N*′-tetramethyl-*p*-phenylenediamine.

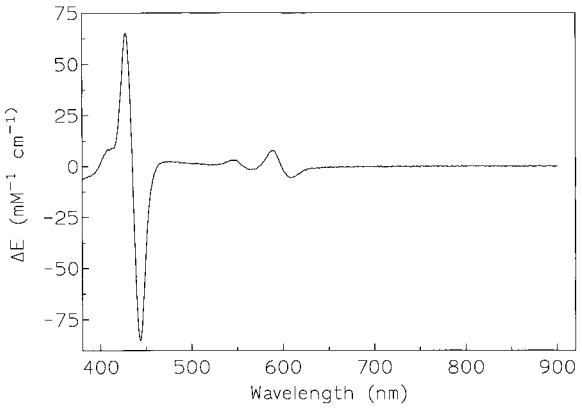

FIGURE 1: Electronic absorption spectrum of the cytochrome *caa*$_3$ complex from *B. subtilis*. Reduced plus CO minus reduced difference spectrum. The enzyme concentration is 5.58 μM in 10 mM sodium phosphate (pH 7.0) with 0.5 mg/mL lauryl maltoside and the CO concentration 1 mM. The spectrum is plotted on a scale of millimolar extinction coefficient based on the extinction coefficient of 26 mM^{-1} cm^{-1} at 604−630 nm for the reduced−oxidized α-band transition of cytochrome *aa*$_3$.

consisting of a 75 W xenon arc lamp and an Applied Photophysics monochromator. The signal intensity was measured using a single photodiode and the output recorded on a Phillips digital oscilloscope and then transferred to the Asystant software package for processing.

RESULTS

We have reported UV−visible absorption spectra for cytochrome *caa*$_3$ in the oxidized and fully reduced states (*26*). Distinct absorption bands are observed for the reduced enzyme at 416 and 550 nm that are typical of ferrocytochrome *c* and at 444 and 604 nm for cytochromes *a* and *a*$_3$. In later kinetic experiments, 550 nm, or 550−540 nm, is used to assess the redox state of cytochrome *c* and 604−630 or 444−460 nm the redox states of cytochromes *a* and *a*$_3$. We have determined that cytochrome *a* contributes 40% to the absorbance at 444−460 nm, whereas 60% arises from cytochrome *a*$_3$ (*26*). At 604−630 nm, 80% of the reduced minus oxidized absorbance intensity is from cytochrome *a* and the remainder from cytochrome *a*$_3$. These values are consistent with those determined for bovine heart mitochondrial cytochrome *c* oxidase (*27*). Figure 1 shows the difference spectrum between fully reduced, CO-bound cytochrome *caa*$_3$ and the fully reduced state as a reference. This spectrum is characterized by peaks at 430 and 590 nm, with troughs at 444 and 610 nm. These features are typical for formation of the ferrocytochrome *a*$_3$−CO complex. Moreover, there are no changes in the region of the cytochrome *c* spectrum that would indicate that CO binds to ferrocytochrome *c*, a reaction which does occur with denatured cytochrome *c* (*28*). We conclude, therefore, that cytochrome *a*$_3$ is the only CO reactive heme in this preparation and that the cytochrome *c* moiety is native and homogeneous from this perspective.

Reduction of Cyanide-Bound Cytochrome caa$_3$. Cyanide binds to the cytochrome *a*$_3$ center of the cytochrome *caa*$_3$ complex (*26*), and we have used the cyanide-bound enzyme to study the kinetics of electron input from the artificial substrates ascorbate and TMPD. Ascorbate alone reduces

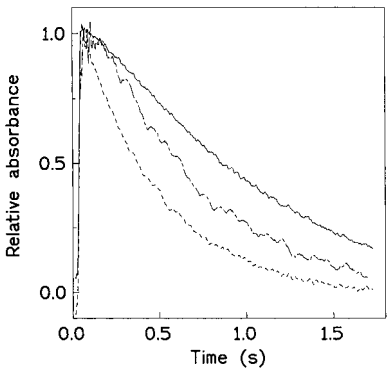

FIGURE 2: Stopped-flow traces of reduction of cyanide-bound cytochrome *caa*$_3$ by ascorbate and TMPD. In each case, the data records include data during the flow period as the old reduced material is washed out of the observation cell. The enzyme concentration was 5 μM in 25 mM sodium phosphate (pH 7.0) with 0.5 mg/mL lauryl maltoside. The enzyme was bound with cyanide by incubation in 1 mM KCN for 30 min prior to reduction by 2.5 mM sodium ascorbate and 50 μM TMPD. Absorbance changes were measured at 550 (—), 790 (− - −), and 604 nm (- -) as a function of time. For ease of comparison, the absorbance has been normalized to 1 by dividing by the total change and the signs of the changes have been made the same by inverting the traces at 604 and 550 nm. The actual absorbance at 550 and 604 nm increases, whereas at 790 nm, the absorbance decreases upon reduction.

cyanide-inhibited cytochrome *caa*$_3$ at a bimolecular rate of 20 M^{-1} s^{-1}. This is slow relative to reduction rates for mammalian cytochrome *c* of 1000 M^{-1} s^{-1} at low ionic strengths but comparable to values obtained at high ionic strengths (*23*). Such slow reactivity with ascorbate presumably reflects the unavailability of a kinetically facile route for electron transfer from ascorbate to the cytochrome *c* domain of subunit II. When ascorbate is supplemented with TMPD, reduction of the cyanide-bound enzyme occurs much more rapidly than the reaction with ascorbate alone. Examples of reduction time courses at 550, 604, and 790 nm, corresponding to the reduction of cytochrome *c*, cytochrome *a*, and Cu$_A$ centers, respectively, are shown in Figure 2. Cytochrome *a* is the fastest species to appear in the reduced state, followed by Cu$_A$ and then cytochrome *c*. In addition, there is a detectable lag at the start of the reduction time course for cytochrome *c*. These features are similar to those reported previously for the reduction of cytochromes *c* and *a* by ascorbate and TMPD in the electrostatic complex formed between mitochondrial cytochrome *c* and cytochrome *c* oxidase (*23*). In this work, we can now include the Cu$_A$ center in the electron-transfer sequence proposed to account for this data. This model proposes the sequence of electron-transfer steps shown below. Cytochrome *c* is reduced initially by TMPD, but this is followed immediately by intramolecular electron transfer from cytochrome *c* to Cu$_A$ and then from Cu$_A$ to cytochrome *a*. Since these internal steps are much faster than the initial electron input from TMPD, reduced cytochrome *c* does not begin to accumulate until relatively late in the reaction.

$$\text{TMPD} \rightarrow c \rightleftarrows \text{Cu}_\text{A} \rightleftarrows a \qquad (1)$$

The rate of reduction of cytochrome *c* by TMPD in such a scheme is the sum of the reduction of the three centers since each is a product of the initial reduction of cytochrome *c*. In

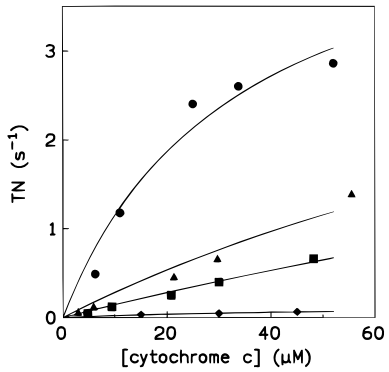

FIGURE 3: Steady-state kinetic properties of cytochrome caa_3 using free cytochrome *c* as a substrate. The assay buffer in each case was 25 mM sodium phosphate (pH 7.0) with 0.5 mg/mL lauryl maltoside at 20 °C with 0.36 μM cytochrome caa_3. The absorbance at 550−540 nm was recorded as a function of time. The time courses followed a single-exponential decrease from which half-times were determined. The observed first-order rate was multiplied by the total cytochrome *c* concentration and divided by the oxidase concentration to give an apparent turnover (TN). The symbols on the graph indicate cytochrome *c* from (●) *B. subtilis*, (▲) *Saccharomyces cerevisiae*, (■) horse heart, and (◆) *Paracoccus denitrificans*. The curves through the points for *B. subtilis* and *P. denitrificans* are fits to the Michaelis−Menten equation.

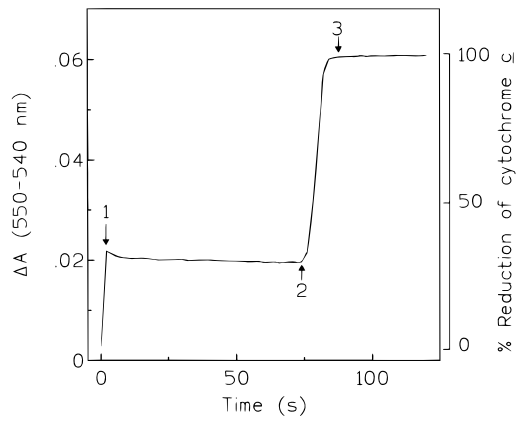

FIGURE 4: Steady-state time course for *B. subtilis* cytochrome caa_3. The enzyme concentration was 2.29 μM in 100 mM sodium phosphate (pH 7.0) with 0.5 mg/mL lauryl maltoside. The absorbance was measured in a diode array spectrometer with spectra taken every 2 s for 120 s. The final concentration of ascorbate was 50 mM and for TMPD 200 μM. The first arrow on the figure is the point of reductant addition, the second arrow the point at which the oxygen is entirely used up, and the third arrow where 100% reduction is obtained.

the example shown in Figure 2, the rate of reduction of cytochrome *c* by TMPD is the rate of appearance of ferrocytochrome *c* plus the rate of appearance of ferrocytochrome *a* plus the rate of appearance of cuprous Cu_A and has a value of 5 s^{-1}. This corresponds to a bimolecular rate of reaction of TMPD with the cytochrome caa_3 complex of 1×10^5 M^{-1} s^{-1}. This is close to the value reported for the reaction of TMPD with the electrostatic cytochrome *c*−cytochrome *c* oxidase complex (*23*).

The above analysis assumes that TMPD puts electrons into the cytochrome caa_3 complex via the cytochrome *c* domain only. It is known that TMPD does reduce mammalian cytochrome *c* oxidase independently of cytochrome *c* (*29*). We have shown previously that binding of cyanide to the cytochrome *c* domain of the caa_3 complex occurs at pHs above 8.0 (*26*). The cyanide-bound cytochrome *c* center in the caa_3 complex cannot be reduced by TMPD but can be reduced by dithionite, similar to mammalian cytochrome *c* (*30*). We find that as the population of cyanide-bound, TMPD nonreducible cytochrome *c* increases so does the fraction of TMPD nonreducible cytochrome *a*, consistent with our proposal that the route of electron entry from TMPD is via the cytochrome *c* domain.

Steady-State Activity with Cytochrome c. The steady-state activity of cytochrome caa_3 may be assessed using ascorbate and TMPD as the electron donor or using ferrocytochrome *c* as the substrate. Figure 3 shows the cytochrome *c* oxidase activity of the cytochrome caa_3 complex with cytochromes *c* from four different organisms. The cytochrome *c* purified from *B. subtilis* is the best substrate relative to the other cytochromes *c* that were tested. The enzyme exhibits saturation behavior with *B. subtilis* cytochrome *c* having a maximal turnover of 5 s^{-1} and a K_M of 33.3 μM. The K_M is in keeping with interaction through a low-affinity site, but the maximal activity is much lower than that obtained with ascorbate and TMPD (see below). *B. subtilis* cytochrome *c* is, however, somewhat unusual compared to mitochondrial cytochrome *c* in having an α-helical domain as a membrane anchor and an acidic isoelectric point (*31*). The integral membrane nature of *B. subtilis* cytochrome *c* means that both proteins in this assay are present as detergent micelles and this may limit their abilities to make productive complexes. Both of the two mitochondrial cytochromes *c* tested here, from horse heart and yeast, exhibit a linear dependence of activity upon concentration (see Figure 3). This linearity is maintained up to 200 μM cytochrome *c*, an indication of very weak binding (i.e., $K_M > 200$ μM) for these proteins. This is not unexpected since the mitochondrial cytochromes *c* are highly basic proteins that are proposed to interact with acidic residues on subunit II of the oxidase and this site is probably occupied by the cytochrome *c* domain of the caa_3 complex. We have also tested, therefore, cytochrome c_{551} from *P. aeruginosa* which is a soluble cytochrome *c*, but has an acidic isoelectric point (*32*). Cytochrome c_{551} exhibits saturation kinetics, but the achieved maximal turnover is very low (i.e., $K_M = 49$ μM, $TN_{max} = 0.13$ s^{-1}).

It is also possible to have steady-state oxygen reduction catalyzed by cytochrome caa_3 using the artificial electron donor combination of ascorbate and TMPD. Steady-state activity was measured both spectrophotometrically and polarographically. In the spectrophotometric assay, the concentration of enzyme is relatively high, allowing the steady-state redox level of the metal centers to be measured, as well as the anaerobiosis time. A typical reaction profile is shown in Figure 4 at 550−540 nm, the wavelengths used to assess the redox status of the cytochrome *c* domain. At time zero, the absorbance level is that of the fully oxidized state and the absorbance jumps to a higher level upon addition of ascorbate and TMPD, which is indicated by the first arrow on the figure. This level remains constant during the steady state until all oxygen is exhausted, whereupon the absorbance again abruptly increases (i.e., at arrow 2) as the cytochrome *c* reaches full reduction, indicated at arrow 3. In the example shown, the steady-state level of cytochrome *c* reduction is 29.4% and the molecular activity 5.82 s^{-1}.

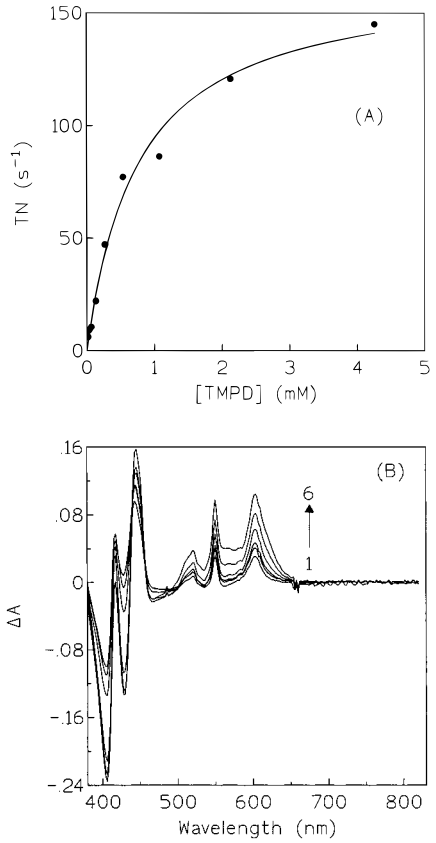

FIGURE 5: Steady-state activity of isolated cytochrome *caa*$_3$. The concentration of enzyme was 2.65 μM, and the ascorbate concentration was 10 mM in 100 mM sodium phosphate (pH 7.0) with 0.5 mg/mL lauryl maltoside. The reaction was initiated by mixing with a Hi-Tech rapid kinetics stopped-flow accessory model SFA-12. (A) The observed rate (TN) is plotted vs TMPD concentration. The rate was determined from the anaerobiosis times, and the ascorbate rate was subtracted from those plus TMPD. (B) Steady-state spectra at different levels of TMPD. A spectrum from the steady-state portion of the time course was taken out of the data set for each concentration of TMPD, and the oxidized spectrum was subtracted. The ascending spectra from 1 to 6 correspond to TMPD concentrations of 0.067, 0.267, 0.533, 2.13, 4.26, and 8.53 mM.

When the enzyme activity is determined as a function of TMPD concentration, it is possible to estimate a K_M and a maximal turnover number. Under the conditions of Figure 5A, the apparent K_M for TMPD is 0.76 mM and the maximal turnover number 166.2 s^{-1}. When spectra of the oxidase recorded during the steady state are examined, the level of reduced cytochrome *c*, apparent at 416 and 550 nm, and cytochrome *a*, at 444 and 604 nm, increases as the concentration of TMPD is increased (see Figure 5B). However, above 1 mM TMPD, another spectral component becomes apparent in the visible region of the spectrum, which disappears when oxygen is exhausted. The properties of this species are consistent with accumulation of a small amount of oxidized TMPD (i.e., TMPD$^{\bullet+}$, the radical cation Wurster's blue). This is presumably due to the inability of ascorbate reduction to keep pace with TMPD oxidation. When the ascorbate level is increased, the signal attributed to TMPD$^{\bullet+}$ is absent and the activity of the oxidase increases. Thus, under the conditions illustrated in Figure 5, the reaction rate limit reached is due to a limit in the reduction of TMPD by ascorbate and is not an intrinsic reaction rate of the oxidase.

The initial conditions employed in this assay were chosen from studies on mitochondrial cytochrome *c* oxidase where typically 5−10 mM ascorbate and 300−600 μM TMPD are sufficient to keep cytochrome *c* fully reduced (*33*). In the case of the cytochrome *caa*$_3$ complex, levels of 10 mM TMPD are required to reach saturating activity, and this requires 250 mM ascorbate so that the reduction of TMPD is not limiting. To use such high levels of sodium ascorbate, we first wanted to investigate the effect that such a high ionic strength would have on the enzyme's activity. We have already reported that in single-turnover experiments measuring the reaction of reduced cytochrome *caa*$_3$ with oxygen observed rates of reactions were unaffected by ionic strength. The steady-state kinetic parameters, K_M and TN_{max}, increase modestly with increased ionic strengths. In 25 mM sodium phosphate, using 10 mM ascorbate and varying TMPD concentrations, a maximal turnover of 50 s^{-1} is observed with a K_M for TMPD of 275 μM. In the same buffer, and 1 M sodium chloride, TN_{max} is 75 s^{-1} with a K_M of 320 μM. In these experiments, the enzyme's activity was determined by measuring rates of O_2 consumption polarographically. The molecular activity parameters determined in this assay, where the concentration of cytochrome *caa*$_3$ is 25−50 nM, are similar to those obtained with the spectrophotometric assay, where the concentration of the enzyme is 2−10 μM. This is often a problem with purified mitochondrial oxidase where the steady-state molecular activity assayed at low enzyme concentrations in the O_2 electrode is not maintained at the high concentrations required to observe spectroscopic properties (*34*).

When the enzyme activity is measured over a wide range of TMPD concentrations (i.e., 10 μM to 10 mM) with a saturating concentration of ascorbate, the limiting steady-state activity of the enzyme can be determined. The data appears to follow simple Michaelis−Menten behavior and begins to reach maximal activity above 5 mM TMPD. However, when the data is viewed (see Figure 6A) in the form of an Eadie−Hofstee plot, its two-component nature is evident. The enzyme exhibits negative cooperativity of substrate affinity and positive cooperativity of activity characterized by a low-activity, high-affinity phase at low TMPD concentrations and a high-activity, low-affinity phase at high TMPD concentrations. The kinetic parameters for the high-affinity phase are as follows: $K_M^1 = 0.228$ mM and $TN_{max}^1 = 23.6$ s^{-1}; for the low-affinity phase, the values are as follows: $K_M^2 = 2.65$ mM and $TN_{max}^2 = 220$ s^{-1}. This result is reminiscent of that obtained in steady-state assays of mitochondrial cytochrome *c* oxidase where the rate is studied as a function of cytochrome *c* concentration (*33*). Two components are also apparent when the extent of reduction of cytochrome *c* and cytochrome *a* is plotted as a function of the TMPD concentration. Figure 6B shows the steady-state level of absorbance at 444−460, 550−540, and 604−630 nm as a fraction of the absorbance at full reduction obtained during anaerobiosis. The band at 444−460 nm has a large contribution from cytochrome a_3, which we presume remains largely oxidized in the steady state, and so it only reaches a level of formation of about 40% at the highest TMPD levels here. At 604−630 nm, the contribution from cytochrome a_3 is only 20% and the signal reaches a level of formation of about 75% at the maximum TMPD used here, corresponding to 90% reduction of cytochrome *a*. The band

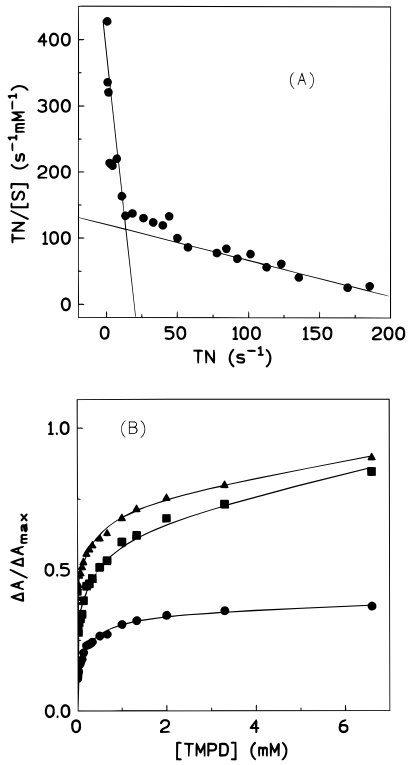

FIGURE 6: Steady-state kinetics of cytochrome caa_3 at an ultrahigh concentration of ascorbate. The concentration of the enzyme was 2.3 μM and that of ascorbate 250 mM in 100 mM sodium phosphate (pH 7.0) with 1 mM EDTA and 0.5 mg/mL lauryl maltoside. (A) Eadie−Hofstee plot of steady-state turnover as a function of TMPD concentration. The straight lines through the data are from a double-hyperbolic fit to the nontransformed data; $TN = TN_{max}^1[S]/(K_M^1 + [S]) + TN_{max}^2[S]/(K_M^2 + [S])$, where TN is the observed turnover, TN_{max}^1 and K_M^1 are the maximal turnover and affinity of the slow phase, respectively, and TN_{max}^2 and K_M^2 are the maximal turnover and affinity of the second, fast phase, respectively. (B) Steady-state reduction levels vs TMPD concentration at the wavelength pairs 444−460 (●), 604−630 (■), and 550−540 nm (▲).

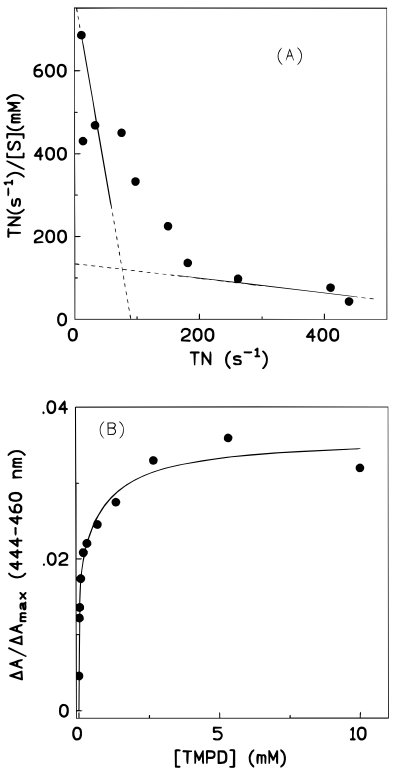

FIGURE 7: Steady-state activity of cytochrome caa_3 in membrane extracts from a *qox*(−) strain. The enzyme concentration was 0.512 μM with 200 mM ascorbate as the reductant in 25 mM sodium phosphate (pH 7.0) with 1 mM EDTA and 0.5 mg/mL lauryl maltoside. (A) Eadie−Hofstee plot of the observed turnover as a function of TMPD concentration. The straight lines through the data are from a double-hyperbolic fit as outlined in the legend of Figure 6A. (B) Steady-state level of reduction at 444−460 nm vs TMPD concentration.

at 550−540 nm, due to cytochrome *c*, reaches a level of reduction of about 85% in this experiment. At low levels of TMPD, there is a steep increase in both the levels of cytochrome *c* and cytochrome *a* reduction in the steady-state up to about 50% which is achieved at about 100 μM TMPD (see Figure 6B).

This two-component steady-state behavior of the cytochrome caa_3 complex could be due to two distinct populations of enzyme present in our preparations. We do not think this is the case for the following reasons. Our preparations of cytochrome caa_3 react homogeneously at the cytochrome a_3 center with both CO and oxygen (*18*), and as we have noted above, the cytochrome *c* domain is fully inert with respect to CO binding in its reduced state as found for native, mitochondrial cytochrome *c*. When the enzyme is assayed spectrophotometrically, as in Figure 4 above, the steady state is level throughout and there is little evidence on this time scale of a resting to "pulsed" conversion as seen with bovine heart oxidase (*34*) and also reported for the cytochrome caa_3 complex from PS3 (*35*). Furthermore, when the steady-state kinetics are determined polarographically at an enzyme concentration 100−500-fold smaller than that used in the spectrophotometric assay, we also observe two components to the activity. One might expect that if this complexity were dependent upon the enzyme's aggregation state that this would be altered in a concentration-dependent manner and so should be manifest over a protein concentration range this wide.

Another possible explanation for the presence of two different forms of the enzyme is that they are products of the isolation procedure. Our purified enzyme is probably variable in its content of the auxiliary subunits III and IV that are encoded by the *cta* operon of *B. subtilis* (*36*). Although there has been no direct correspondence made for the presence of these subunits in vitro and either electron or proton translocation activities for any of the enzymes of the cytochrome oxidase family, we decided to look at the activity of the cytochrome caa_3 in the initial membrane extract. This experiment is complicated in wild-type *B. subtilis* by the presence of a second heme A containing terminal oxidase, the cytochrome aa_3 (600 nm) menaquinol oxidase. Therefore, we prepared membrane extracts from a strain of *B. subtilis* in which expression of the menaquinol oxidase is disrupted (X. Shao and B. C. Hill, unpublished results). The cytochrome caa_3 steady-state activity exhibited in these extracts is illustrated in Figure 7. Figure 7A shows an Eadie−Hofstee plot of enzyme activity, and Figure 7B shows the steady-state absorbance level at 444−460 nm as the TMPD concentration is increased. The biphasic nature exhibited at the initial extract stage supports the proposal that this is an inherent property of the enzyme and does not arise as an artifact of its purification.

DISCUSSION

The cytochrome *c* domain of cytochrome caa_3 appears to have the same reactivity as the cytochrome *c* molecule in the mammalian cytochrome *c*−cytochrome aa_3 complex that is stabilized at low ionic strengths. In the reaction of fully reduced cytochrome caa_3, of either mitochondrial or bacterial origin, the cytochrome *c* moiety donates an electron early in the reaction sequence because of its high reactivity with Cu_A (*18*, *19*, *37*). The same reaction sequence can be used to understand the reduction of oxidized, cyanide-bound *B. subtilis* cytochrome caa_3. Electron input into cytochrome *c* is followed by electron transfer to Cu_A and thence to cytochrome *a*, and this sequence of reactivity appears to be the same as in the mammalian complex (*23*). Since the reactivity of the cytochrome *c* domain is in many ways the same as that of tightly bound cytochrome *c* in the electrostatic cytochrome *c*−cytochrome *c* oxidase complex, we propose that it has the same disposition relative to the other metal centers of the oxidase. Thus, the cytochrome *c* domain that is an extension of subunit II in the *B. subtilis* cytochrome caa_3 complex is equivalent to tightly bound cytochrome *c* in the mammalian cytochrome *c*−cytochrome oxidase complex.

The underlying reason for the biphasic behavior of cytochrome *c* oxidase in steady-state assays has been the subject of numerous proposals. Initially, biphasic kinetics was interpreted in terms of two binding sites for cytochrome *c* with two intrinsic stability constants associated with two different enzymatic turnovers (*21*). Alternatively, Speck et al. (*38*) have suggested that biphasic kinetics can be explained if there is a single catalytic site for cytochrome *c* from which product dissociation becomes limiting. Binding of cytochrome *c* to secondary, nonproductive sites can promote dissociation of cytochrome *c* from the catalytic site and thereby promote turnover. In the case of the cytochrome caa_3 complex from *B. subtilis*, there is only a single type of interaction with cytochrome *c* when oxidizing ascorbate and TMPD are present. This interaction is covalent in nature and fixes the cytochrome *c* into a homogeneous structural and functional disposition. We suggest, therefore, that models which require multiple binding sites for cytochrome *c* or changes in the nature of the cytochrome *c* interaction to account for the multiphasic steady-state kinetics are not required to explain the biphasic kinetics observed here.

Ortega-Lopez and Robinson (*39*) studied the steady-state kinetics of the bovine enzyme at different levels of TMPD in different detergents. These authors propose that the low-activity phase in the steady-state kinetics results from limited electron input to cytochrome *a* and that this limitation is relieved by excess cytochrome *c* which yields the low-affinity, high-activity phase. In contrast, in the experiments reported here, we have only a single path of electron input to cytochrome *a*, and this does not change as a function of the reduction rate. The observation here of a biphasic progression in the redox level of cytochrome *a* as a function of turnover, therefore, results from changes in the rate of electron output from cytochrome *a*. We ascribe this change in electron output rate from cytochrome *a* to changes in the conformational state of the protein. These conformational forms are not necessarily an inherent structural feature of the enzyme but arise as a feature of the catalytic cycle.

The basic properties of a conformational model of cytochrome *c* oxidase steady-state kinetics have been outlined previously by Malmström and co-workers (*22*, *40*, *41*). These workers have pointed out the obligatory role of conformational changes in coupling proton pumping to electron transfer (*41*). Cytochrome oxidases of the caa_3 type have also been shown to function as proton pumps (e.g., from *T. thermophilus*; *42*), and we have preliminary evidence of proton pumping from purified, reconstituted *B. subtilis* cytochrome caa_3 (I. Perin, P. Nicholls, and B. C. Hill, unpublished observations). Spectral evidence of different conformers of the oxidase in different redox states has been observed in UV−CD measurements of bovine oxidase (*43*). However, FTIR spectra of the oxidase in different redox states reveal only very small scale conformational changes (*44*). We suggest that the data presented here offer support for the manifestation of conformational changes as a part of the catalytic cycle of the oxidase. In the model developed by Malmström, the conformation is linked to the redox status and/or the protonation state of a catalytic center or centers of the enzyme. At present, we cannot distinguish which of these possibilities, or some other, is more likely as a feasible explanatory model. Biphasic steady-state kinetics have also recently been reported for the cytochrome caa_3 from *T. thermophilus* as a function of TMPD concentration (*45*). In addition, biphasicity in the reduction of cytochrome *a* has been reported in steady-state assays of cytochrome *c* oxidase in situ, in intact rat liver mitochondria, using ascorbate and TMPD to deliver electrons to cytochrome *c* (*46*). We suggest that the biphasic nature of the steady-state kinetics of cytochrome oxidase is independent of cytochrome *c* and is a feature of cytochrome oxidases in general. The biphasic behavior is due to conformational forms of the oxidase that have different maximal turnovers.

The covalent attachment of cytochrome *c* via subunit II to the oxidase unit in the *B. subtilis* caa_3 complex raises the issue of the natural reducing substrate. There is a free cytochrome *c* that is expressed in wild-type *B. subtilis* that behaves as a substrate for the cytochrome caa_3 complex. However, we have determined here that it is only a poor reductant of the caa_3 complex in vitro. The free cytochrome *c* of *B. subtilis* is, like its oxidase, an integral membrane protein, and this may introduce rate-limiting constraints on the reactivity of the isolated proteins. In the reactions reported here, both the purified cytochrome *c* and the cytochrome caa_3 complex were present in the steady-state assay as detergent micelles. Despite these constraints, the *B. subtilis* cytochrome *c* was still the most efficient of the cytochromes *c* tested. It is likely that the reactivity of these two membrane proteins would be enhanced greatly when present within the same membrane bilayer. The free *B. subtilis* cytochrome *c* might be the natural reductant of the cytochrome caa_3 complex despite its poor performance relative to ascorbate and TMPD in vitro. Alternatively, the cytochrome bc_1 complex of *B. subtilis* might be able to deliver electrons directly to the cytochrome *c* domain of the caa_3. This is an interesting possibility that we are pursuing at present.

REFERENCES

1. Ferguson-Miller, S., and Babcock, G. T. (1996) *Chem. Rev. 96*, 2889−2907.

2. Saraste, M. (1994) *Antonie van Leeuwenhoek 65*, 285−287.
3. Tsukihara, T., Aoyama, H., Yamashita, E., Tomizaki, T., Yamaguchi, H., Shinzawa-Itoh, K., Nakashima, R., Yaono, R., and Yoshikawa S. (1996) *Science 272*, 1136−1144.
4. Wikström, M., Bogachev, A., Finel, M., Morgan, J., Puustinen, A., Raitio, M., Verkhovskaya, M., and Verkhovsky, M. I. (1994) *Biochim. Biophys. Acta 1187*, 106−111.
5. Riistama, S., Hummer, G., Puustinen, A., Dyer, R. B., Woodruff, W. H., and Wikström, M. (1997) *FEBS Lett. 414*, 275−280.
6. Hill, B. C., Vo, L., and Albanese, J. (1993) *Arch. Biochem. Biophys. 301*, 129−137.
7. Sone, N., Ohyama, T., and Kagawa, Y. (1979) *FEBS Lett. 106*, 36−42.
8. Fee, J. A., Choc, M. G., Findling, K. L., Lorence, R., and Yoshida, T. (1980) *Proc. Natl. Acad. Sci. U.S.A. 77*, 147−151.
9. Quirk, P. G., Hicks, D. B., and Krulwich, T. A. (1993) *J. Biol. Chem. 268*, 678−685.
10. Hill, B. C. (1991) *J. Biol. Chem. 266*, 2219−2226.
11. Hill, B. C. (1993) *J. Bioenerg. Biomembr. 25*, 115−120.
12. Varotsis, C., Zhang, Y., Appelman, E. H., and Babcock, G. T. (1993) *Proc. Natl. Acad. Sci. U.S.A. 90*, 237−241.
13. Boelens, R., Wever, R., and van Gelder, B. F. (1982) *Biochim. Biophys. Acta 682*, 264−272.
14. Verkhovsky, M. I., Morgan, J., and Wikström, M. (1992) *Biochemistry 31*, 11860−11863.
15. Nilsson, T. (1992) *Proc. Natl. Acad. Sci. U.S.A. 89*, 6497−6501.
16. Pan, L. P., Hibdon, S., Liu, R.-Q., Durham, B., and Millet, F. (1993) *Biochemistry 32*, 8492−8498.
17. Geren, L. M., Beasley, J. R., Fine, B. R., Suanders, A. J., Hibdon, S., Pielak, G. J., Durham, B., and Millet, F. (1995) *J. Biol. Chem. 270*, 2466−2472.
18. Hill, B. C. (1996) *Biochemistry 35*, 6136−6143.
19. Hill, B. C. (1994) *J. Biol. Chem. 269*, 2419−2425.
20. Cooper, C. E. (1990) *Biochim. Biophys. Acta 1017*, 187−203.
21. Nicholls, P. (1964) *Arch. Biochem. Biophys. 106*, 25−48.
22. Malmström, B. G. (1985) *Biochim. Biophys. Acta 811*, 1−12.
23. Hill, B. C., and Nicholls, P. (1980) *Biochem. J. 187*, 809−818.
24. Henning, W., Vo, L., Albanese, J., and Hill, B. C. (1995) *Biochem. J. 309*, 279−283.
25. Smith, L., and Conrad, H. (1956) *Arch. Biochem. Biophys. 63*, 403−413.
26. Assempour, M., and Hill, B. C. (1997) *Biochim. Biophys. Acta 1320*, 175−187.
27. Liao, G.-L., and Palmer, G. (1996) *Biochim. Biophys. Acta 1274*, 109−111.
28. Tsou, C. L. (1951) *Biochem. J. 49*, 362−367.
29. Kimelberg, H. K., and Nicholls, P. (1969) *Arch. Biochem. Biophys. 133*, 327−335.
30. Brooks, S. P. J., Chanady, G. A., and Nicholls, P. (1982) *Can. J. Biochem. 60*, 763−770.
31. von Wachenfeldt, C., and Hederstedt, L. (1990) *J. Biol. Chem. 265*, 13939−13948.
32. Meyer, T. E., and Kamen, M. D. (1982) *Adv. Protein Chem. 35*, 105−212.
33. Ferguson-Miller, S., Brautigan, D. L., and Margoliash, E. (1978) *J. Biol. Chem. 253*, 149−159.
34. Nicholls, P., Hildebrandt, V., Hill, B. C., Nicholls, F., and Wrigglesworth, J. M. (1980) *Can. J. Biochem. 58*, 969−977.
35. Sone, N., Naqui, A., Kumar, C., and Chance, B. (1984) *Biochem. J. 223*, 809−813.
36. Saraste, M., Metso, T., Nakari, T., Jalli, T., Lauraeus, M., and Van der Oost, J. (1991) *Eur. J. Biochem. 195*, 517−525.
37. Hirota, S., Svensson-Ek, M., Ädelroth, P., Sone, N., Nilsson, T., Malmström, B. G., and Brzezinski, P. (1996) *J. Bioenerg. Biomembr. 28*, 495−501.
38. Speck, S. H., Dye, D., and Margoliash, E. (1984) *Proc. Natl. Acad. Sci. U.S.A. 81*, 347−351.
39. Ortega-Lopez, J., and Robinson, N. C. (1995) *Biochemistry 34*, 10000−10008.
40. Brzezinski, P., Thörnström, P.-E., and Malmström, B. G. (1986) *FEBS Lett. 194*, 1−5.
41. Brzezinski, P., and Malmström, B. G. (1986) *Proc. Natl. Acad. Sci. U.S.A. 83*, 4282−4286.
42. Hon-nami, K., and Oshima, T. (1984) *Biochemistry 23*, 454−460.
43. Wittung, P., and Malmström, B. G. (1996) *FEBS Lett. 388*, 47−49.
44. Hellwig, P., Rost, B., Kaiser, U., Ostermeier, C., Michel, H., and Mantele, W. (1996) *FEBS Lett. 385*, 53−57.
45. Soulimane, T., von Walter, M., Hof, P., Than, M. E., Huber, R., and Buse, G. (1997) *Biochem. Biophys. Res. Commun. 237*, 572−576.
46. Morgan, J. E., and Wikström, M. (1991) *Biochemistry 30*, 948−958.

BI980331C